Inorganic Chemistry

ARTICLE

pubs.acs.org/IC

$Ba_3[Ge_2B_7O_{16}(OH)_2](OH)(H_2O)$ and $Ba_3Ge_2B_6O_{16}$: Novel Alkaline-Earth Borogermanates Based on Two Types of Polymeric Borate Units and GeO_4 Tetrahedra

Jian-Han Zhang,[†,‡] Fang Kong,[†] and Jiang-Gao Mao*[,†]

[†]State Key Laboratory of Structural Chemistry, Fujian Institute of Research on the Structure of Matter, Chinese Academy of Sciences, Fuzhou 350002, People's Republic of China

[‡]Graduate School of the Chinese Academy of Sciences, Beijing, 100039, People's Republic of China

Supporting Information

ABSTRACT: Two new barium borogermanates with two types of novel structures, namely, $Ba_3[Ge_2B_7O_{16}(OH)_2](OH)(H_2O)$ and $Ba_3Ge_2B_6O_{16}$, have been synthesized by hydrothermal or high-temperature solid-state reactions. They represent the first examples of alkaline-earth borogermanates. $Ba_3[Ge_2B_7O_{16}(OH)_2](OH)(H_2O)$ crystallized in a polar space group *Cc*. Its structure features a novel three-dimensional anionic framework composed of $[B_7O_{16}(OH)_2]^{13-}$ polyanions that are bridged by Ge atoms with one-dimensional (1D) 10-membered-ring (MR) tunnels along the *b* axis. The Ba^{II} cations, hydroxide ions, and water molecules are located at the above tunnels. $Ba_3Ge_2B_6O_{16}$ crystallizes in centrosymmetric space group $P\bar{1}$. Its structure exhibits a thick layer composed of circular B_6O_{16} units connected by GeO_4 tetrahedra via corner sharing, forming 1D 4- and 6-MR tunnels along the *c* axis. Ba1 ions reside in the tunnels of the 6-MRs, whereas Ba2 ions are located at the interlayer space. Both compounds feature new types of topological structures. Second-harmonic-generation (SHG) measurements indicate that $Ba_3[Ge_2B_7O_{16}(OH)_2](OH)(H_2O)$ displays a weak SHG response of about 0.3 times that of KH_2PO_4. Optical, thermal stability, and ferroelectric properties as well as theoretical calculations have also been performed.

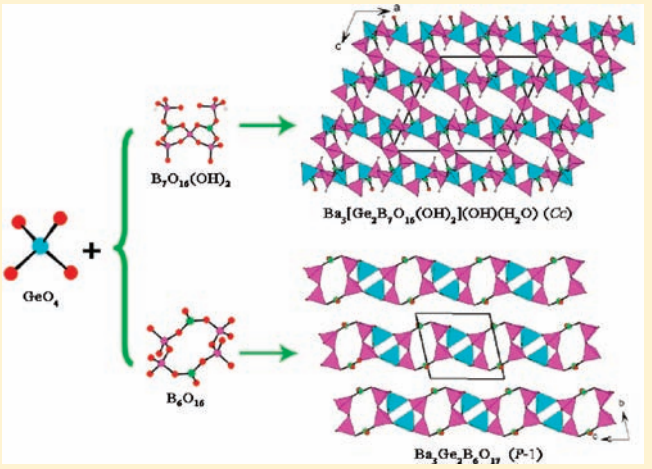

INTRODUCTION

Metal borates and germanates play important roles in nonlinear optical and porous materials, respectively.[1−3] The combination of the borate and germanate groups in the same crystalline material has generated a new class of materials, metal borogermanates. Though reports on metal borogermanates are still limited, they are able to form various noncentrosymmetric structures with possible second-harmonic-generation (SHG) properties or zeolite-type open frameworks.[4−13] A series of organically templated layered or three-dimensional (3D) borogermanates have been reported by the Zou and Yang groups.[4,5] It is found that the size, shape, and charge of the template cations may direct the formation of different open frameworks. Several types of lanthanide(III) borogermanates have also been reported,[6−9] among which $Ln_{14}(GeO_4)_2(BO_3)_6O_8$ and $LnGeBO_5$ ($P3_1$) are structurally acentric.[8,9a] Unfortunately, their SHG properties were not studied.

A series of alkali borogermanates have been synthesized, including $KBGe_2O_6$,[10a] $K_2[GeB_4O_9]\cdot 2H_2O$,[10b] $CsGeB_3O_7$, $K_2B_2Ge_3O_{10}$,[11] $LiBGeO_4$,[12] $K_4[B_8Ge_2O_{17}(OH)_2]$,[13a] and $NH_4(BGe_3O_8)$.[13b] They display several types of open-framework structures, and, more interestingly, $K_2GeB_4O_9\cdot 2H_2O$ and $CsGeB_3O_7$ exhibit moderate SHG responses that are 2.0 and 1.5 times of that of KH_2PO_4 (KDP), respectively.[10b,11] The structure of $KBGe_2O_6$ features a 3D network composed of one-dimensional (1D) chains of corner-sharing GeO_4 tetrahedra interconnected by BO_4 tetrahedra, forming 7-membered ring (MR) tunnels that are filled with K^I ions.[10a] The 3D structure of $K_2[GeB_4O_9]\cdot 2H_2O$ is based on B_4O_9 units corner-sharing with GeO_4 tetrahedra, whereas $CsGeB_3O_7$ features a novel 3D framework composed of cyclic B_3O_7 groups corner-sharing with GeO_4 tetrahedra.[10b,11] The structure of $K_2B_2Ge_3O_{10}$ is a 3D network based on cap-shaped $[Ge_3B_2O_{14}]^{10-}$ units that are interconnected via Ge−O−B bridges, forming 1D 8-MR tunnels.[11] The layered $K_4[B_8Ge_2O_{17}(OH)_2]$ displays 3D microporosity within the layer.[12a] $NH_4BGe_3O_8$ shows a 3D structure with 1D 10-MR tunnels based on 1D $\{Ge_6O_{18}\}_n$ chains with alternating 4- and

Received: December 24, 2010
Published: March 09, 2011

   dx.doi.org/10.1021/ic1025697 | *Inorg. Chem.* 2011, 50, 3037–3043

6-MRs made of vertex-sharing GeO_4 tetrahedra, which are further linked with BO_4 tetrahedra.[12b] $LiBGeO_4$ crystallized in space group $I\bar{4}$ and features a 3D network with 6-MR tunnels in which the corner-sharing BO_4 and GeO_4 tetrahedra are strictly alternating.[13]

So far, no alkaline-earth borogermanate has been reported. We deem that the different charges and ionic sizes of alkaline-earth cations compared with alkali cations may lead to new borogermanates with different open frameworks and physical properties. Furthermore, it is assumed that the different synthetic methods and B/Ge ratios applied may lead to different boron−oxygen units and different connectivity fashions with the GeO_4 tetrahedra. Therefore, we started a research program to explore alkaline-earth borogermanates as new potential SHG materials.

EXPERIMENTAL SECTION

Materials and Methods. H_3BO_3 (Shanghai Reagent Factory, 99.9%), GeO_2 (Shanghai Reagent Factory, 99.99%), and $BaCO_3$(Alfa Aesar, 99.0%) were used without further purification. IR spectra were recorded on a Magna 750 FT-IR spectrometer as KBr pellets in the range of 4000−400 cm^{-1}. Microprobe elemental analyses for the Ba and Ge elements were performed on a field-emission scanning electron microscope (JSM6700F) equipped with an energy-dispersive X-ray spectroscope (Oxford INCA). Powder X-ray diffraction (XRD) patterns were collected on a XPERT-MPD $\theta-2\theta$ diffractometer using graphite-monochromated Cu Kα radiation in the 2θ range of 5−85° with a step size of 0.05°. Optical diffuse-reflectance spectra were measured at room temperature with a PE Lambda 900 UV−visible spectrophotometer. The $BaSO_4$ plate was used as a standard (100% reflectance). The absorption spectrum was calculated from reflectance spectrum using the Kubelka−Munk function: $\alpha/S = (1 - R)^2/2R$,[14] where α is the absorption coefficient, S is the scattering coefficient, which is practically wavelength-independent when the particle size is larger than 5 μm, and R is the reflectance. Thermogravimetric analysis (TGA) was carried out with a NETZSCH STA 449C unit at a heating rate of 15 °C/min under an oxygen atmosphere. Measurements of the powder frequency-doubling effect were carried out by means of the modified method of Kurtz and Perry.[15] A 1064 nm radiation generated by a Q-switched Nd:YAG solid-state laser was used as the fundamental frequency light. The SHG wavelength is 532 nm. The SHG efficiency has been shown to depend strongly on the particle size; thus, the sample was ground and sieved into several distinct particle size ranges (25−45, 45−53, 53−75, 75−105, 105−150, and 150−210 μm). Sieved KDP powder (150−210 μm) was used as a reference material to assume the SHG effect. The ferroelectric measurements for $Ba_3[Ge_2B_7O_{16}(OH)_2](OH)(H_2O)$ were performed on an aixACCT TF Analyzer 2000 ferroelectric tester at room temperature. The sample was pressed into a pellet (5 mm diameter and 0.6 mm thickness), and the conducting silver glue was applied on both sides of the pellet.

Synthesis of $Ba_3[Ge_2B_7O_{16}(OH)_2](OH)(H_2O)$. A mixture of $BaCO_3$ (0.148 g, 0.75 mmol), GeO_2(0.052 g, 0.5 mmol), H_3BO_3 (0.108 g, 1.75 mmol), and H_2O (2.0 mL) was sealed in an autoclave equipped with a Teflon liner (23 mL) and heated at 200 °C for 4 days, followed by slow cooling to room temperature at a rate of 6 °C/h. The initial and final pH values are 5.5 and 7.5, respectively. The product was washed with hot water and ethanol and then dried in air. The final product is mainly colorless hexagon tile-shaped crystals of $Ba_3[Ge_2B_7O_{16}(OH)_2](OH)(H_2O)$ with a small amount of white powder of $BaGeO_3$ as an impurity. A number of things were tried to prepare a single phase of $Ba_3[Ge_2B_7O_{16}(OH)_2](OH)(H_2O)$, such as changing the pH values, reaction times, and temperatures; however, a small amount of white powder of $BaGeO_3$ was always present as an impurity. Finally, a single phase of $Ba_3[Ge_2B_7O_{16}(OH)_2](OH)(H_2O)$ was isolated in a yield of ca. 85% based on Ba after sieving by ultrasound. Its purity was confirmed by a powder XRD study (Figure S6a in the Supporting Information). Energy-dispersive spectrometry (EDS) elemental analyses on several single crystals of $Ba_3[Ge_2B_7O_{16}(OH)_2](OH)(H_2O)$ gave an average molar ratio of Ba:Ge of 2.9:2.0, which is in good agreement with that determined from single-crystal X-ray structural studies. IR data (KBr, cm^{-1}): 3161(s), 1626(m), 1399(s), 1258(m), 1131(m), 1044(s), 916(s), 837(s), 655(w), 579(w), 490(w).

Synthesis of $Ba_3Ge_2B_6O_{16}$. Colorless block-shaped single crystals of $Ba_3Ge_2B_6O_{16}$ were initially obtained by high-temperature solid-state reactions of a mixture of $BaCO_3$ (0.5919 g, 3 mmol), GeO_2 (0.2072 g, 2 mmol), and H_3BO_3 (0.3708 g, 6 mmol). The reaction mixture was thoroughly ground in an agate mortar and then transferred to a platinum crucible. The sample was heated at 800 °C for 4 days and then cooled to 200 °C at a cooling rate of 2.4 °C/h before the furnace was switched off. The average atomic ratio of Ba:Ge determined by EDS on several single crystals of each compound is 3.0:2.1, which is in good agreement with that from structural analysis. After proper crystal structure determination, a colorless crystalline sample of $Ba_3Ge_2B_6O_{16}$ was obtained quantitatively by the reaction of a mixture of $BaCO_3/GeO_2/H_3BO_3$ in a molar ratio of 3:2:3 at 800 °C for 5 days. Its purity was confirmed by power XRD studies (Figure S3b in the Supporting Information). IR data (KBr, cm^{-1}): 1375(s), 1228(m), 1063(s), 925(s), 868(s), 832(s), 770(m), 609(m), 584(m), 460(w).

Single-Crystal Structure Determination. Data collections for the two compounds were performed on either a Rigaku Mercury 70 [for $Ba_3[Ge_2B_7O_{16}(OH)_2](OH)(H_2O)$] or a Rigaku Mercury 2 CCD diffractometer (for $Ba_3Ge_2B_6O_{16}$) equipped with graphite-monochromated Mo Kα radiation (λ = 0.710 73 Å) at 293(2) K. Both data sets were corrected for Lorentz and polarization factors as well as for absorption by a multiscan method.[16a] Both structures were solved by direct methods and refined by a full-matrix least-squares fitting on F^2 by *SHELX-97*.[16b] All of the non-H atoms were refined with anisotropic thermal parameters except O1, O6, and B3−B7 in $Ba_3[Ge_2B_7O_{16}(OH)_2](OH)(H_2O)$, which were refined isotropically. The date set of $Ba_3[Ge_2B_7O_{16}(OH)_2](OH)(H_2O)$ was performed in TWIN refinements. The Flack factor of 0.51(2) indicates the existence of racemic twinning. This is proven by the refinements of several data sets collected on different crystals. O5 and O11 of the Ge−B−O framework and O1H are singly protonated, whereas O1w is an aqua ligand based on the requirement of charge balance and bond-valence calculations; their calculated bond valences are −1.03, −1.07, −1.3, and −0.4, respectively.[17] All H atoms except those for an aqua ligand in $Ba_3[Ge_2B_7O_{16}(OH)_2](OH)(H_2O)$ were located at geometrically calculated positions and refined with isotropic thermal parameters. H atoms for water molecules were not included in the refinements. We have also tried to solve this structure in the centrosymemtric space group $C2/c$, but R1 (about 0.102) is too high and many atoms are nonpositive-definite. Therefore, we finally chose space group Cc, which gave a satisfactory refinement with R1 = 0.029 for 3306 unique reflections with $I > 2\sigma(I)$. Crystallographic data and structural refinements for the two compounds are summarized in Table 1. Important bond distances are listed in Table 2. More details on the crystallographic studies as well as atomic displacement parameters are given as Supporting Information.

Computational Descriptions. Single-crystal structural data of both compounds were used for their electronic and optical property calculations. Band structures and density of states (DOS) were performed with the total energy code CASTEP.[18] The total energy is calculated with density functional theory using the Perdew−Burke−Ernzerhof generalized gradient approximation (GGA).[19] The interactions between the ionic cores and the electrons are described by the norm-conserving pseudopotential.[20] The following orbital electrons are treated as valence electrons: Ba $5p^6 6s^2$, Ge $4s^2 4p^2$, B $2s^2 2p^1$, and

dx.doi.org/10.1021/ic1025697 |*Inorg. Chem.* 2011, 50, 3037–3043

Table 1. Crystal Data and Structure Refinements for $Ba_3[Ge_2B_7O_{16}(OH)_2](OH)(H_2O)$ and $Ba_3Ge_2B_7O_{16}$

formula	$Ba_3[Ge_2B_7O_{16}(OH)_2](OH)(H_2O)$	$Ba_3Ge_2B_7O_{16}$
fw	957.91	878.07
Space group	*Cc*	$P\bar{1}$
a (Å)	14.805(7)	5.0923(5)
b (Å)	8.516(4)	7.5996(6)
c (Å)	13.51(1)	8.5973(7)
α (deg)	90	77.50(2)
β (deg)	113.942(5)	77.53(2)
γ (deg)	90	88.17(2)
V (Å^3)	1557.3(15)	317.12(5)
Z	4	1
D_c (g cm^{-3})	4.086	4.598
μ(Mo Kα) (mm^{-1})	11.407	13.960
GOF on F^2	1.034	1.062
Flack factor	0.51(2)	none
R1, wR2 [$I > 2\sigma(I)$][a]	0.0288, 0.0675	0.0348, 0.0815
R1, wR2 (all data)[a]	0.0297, 0.0684	0.0370, 0.0833

[a] $R1 = \Sigma||F_o| - |F_c||/\Sigma|F_o|$, $wR2 = \{\Sigma w[(F_o)^2 - (F_c)^2]^2/\Sigma w[(F_o)^2]^2\}^{1/2}$.

O $2s^22p^4$. The number of plane waves included in the basis set is determined by a cutoff energy of 500 eV, and the numerical integration of the Brillouin zone is performed using a $3 \times 3 \times 2$ and $5 \times 3 \times 3$ Monkhorst–Pack *k*-point sampling for $Ba_3[Ge_2B_7O_{16}(OH)_2](OH)(H_2O)$ and $Ba_3Ge_2B_6O_{16}$, respectively. The other calculating parameters and convergent criteria were the default values of the CASTEP code.

RESULTS AND DISCUSSION

Explorations of alkaline-earth borogermanates in the Ba–Ge–B–O system led to two new compounds, namely, $Ba_3[Ge_2B_7O_{16}(OH)_2](OH)(H_2O)$ and $Ba_3Ge_2B_6O_{16}$. They represent the first structurally characterized alkaline-earth borogermanates. It is interesting to note that $Ba_3[Ge_2B_7O_{16}(OH)_2](OH)(H_2O)$ and $Ba_3Ge_2B_6O_{16}$ were synthesized in similar molar ratios of reactants by using different synthetic methods. $Ba_3[Ge_2B_7O_{16}(OH)_2](OH)(H_2O)$ was synthesized hydrothermally, whereas $Ba_3Ge_2B_6O_{16}$ was synthesized by a high-temperature solid-state reaction. Hence, the synthetic method used has a dramatic effect on the chemical compositions and structures of the compounds formed. $Ba_3[Ge_2B_7O_{16}(OH)_2](OH)(H_2O)$ and $Ba_3Ge_2B_6O_{16}$ feature two types of anionic open frameworks based on two types of polymeric borate units ($B_7O_{16}(OH)_2$ and B_6O_{16}) interconnected by GeO_4 tetrahedra.

The structure of $Ba_3[B_7Ge_2O_{16}(OH)_2](OH)(H_2O)$ crystallizes in the polar space group *Cc* (No. 9). It belongs to a new structure type, and its structure features a unique 3D anionic framework composed of $[B_7O_{16}(OH)_2]^{13-}$ polyanions corner-sharing with GeO_4 tetrahedra, forming 1D 10-membered ring (MR) tunnels along the *b* axis that are occupied by Ba^{2+} cations, hydroxide anions, and water molecules (Figure 1a). The asymmetric unit of $Ba_3[B_7Ge_2O_{16}(OH)_2](OH)(H_2O)$ contains three Ba, two Ge, and seven B atoms. Both Ge^{IV} atoms are tetrahedrally coordinated by four O atoms, with Ge–O distances ranging from 1.727(5) to 1.756(5) Å and O–Ge–O bond angles in the range of 101.5(2)–116.9(2)°. B1, B2, B3, B4, and B5 are tetrahedrally coordinated, whereas B6 and B7 are in a triangular BO_3 geometry. The B–O bond distances of the BO_3 group [1.35(1)–1.40(1) Å] are significantly shorter than those of BO_4 or $BO_3(OH)$ tetrahedra [1.43(1)–1.507(9) Å]. The O–B–O angles are in the ranges of 114.0(8)–124.2(7)° for triangular BO_3 units and 105.2(5)–115.5(5)° for BO_4 tetrahedra. All of these bond distances and angles are comparable to those reported in other metal borogermanates.[4–13]

Table 2. Important Bond Lengths (Å) for $Ba_3[Ge_2B_7O_{16}(OH)_2](OH)(H_2O)$ and $Ba_3Ge_2B_7O_{16}$[a]

$Ba_3[Ge_2B_7O_{16}(OH)_2](OH)(H_2O)$			
Ge1–O7	1.736(5)	Ge1–O2	1.750(5)
Ge1–O9#1	1.754(5)	Ge1–O1	1.756(5)
Ge2–O15#2	1.727(5)	Ge2–O4	1.732(5)
Ge2–O12	1.751(5)	Ge2–O16#3	1.753(5)
B1–O17	1.426(10)	B1–O13#1	1.477(10)
B1–O16	1.501(10)	B1–O1	1.507(9)
B2–O18	1.452(10)	B2–O8	1.453(10)
B2–O15	1.488(8)	B2–O9	1.495(10)
B3–O18	1.454(9)	B3–O17#3	1.456(9)
B3–O14#2	1.466(10)	B3–O10#4	1.483(11)
B4–O11#5	1.454(9)	B4–O7#6	1.468(9)
B4–O6	1.486(9)	B4–O12#6	1.501(8)
B5–O5	1.458(9)	B5–O4	1.477(9)
B5–O3	1.492(9)	B5–O2	1.501(8)
B6–O10#1	1.352(12)	B6–O3	1.359(10)
B6–O8#7	1.401(10)	B7–O14	1.361(12)
B7–O6	1.365(11)	B7–O13	1.382(11)
$Ba_3Ge_2B_7O_{16}$			
Ge1–O4#1	1.718(4)	Ge1–O2	1.732(5)
Ge1–O3	1.734(4)	Ge1–O1#2	1.753(5)
B1–O5	1.453(9)	B1–O1	1.458(8)
B1–O8	1.480(8)	B1–O3	1.496(8)
B2–O5	1.439(9)	B2–O4	1.476(8)
B2–O7#3	1.484(9)	B2–O2#4	1.512(8)
B3–O6	1.327(8)	B3–O7#5	1.390(8)
B3–O8#6	1.415(9)		

[a] Symmetry transformations used to generate equivalent atoms. For $Ba_3[Ge_2B_7O_{16}(OH)_2](OH)(H_2O)$: #1, $x, -y+1, z+{}^1/_2$; #2, $x+{}^1/_2, -y+{}^3/_2, z+{}^1/_2$; #3, $x+{}^1/_2, y+{}^1/_2, z$; #4, $x, y+1, z$; #5, $x-{}^1/_2, y-{}^1/_2, z$; #6, $x-{}^1/_2, -y+{}^1/_2, z-{}^1/_2$; #7, $x, -y+2, z+{}^1/_2$. For $Ba_3Ge_2B_7O_{16}$: #1, $-x+1, -y+1, -z+1$; #2, $x-1, y, z$; #3, $-x+2, -y+1, -z+1$; #4, $x+1, y, z$; #5, $x-1, y, z-1$; #6, $x-1, y, z$.

Two triangular BO_3 groups (B6 and B7) and three BO_4 tetrahedra (B1, B2, and B3) are interconnected via corner sharing to form a B_5O_{12} unit with two approximately perpendicular 3-MRs. The dihedral angle between these two 3-MRs is 89.3(3)°. Two $BO_3(OH)$ groups (B4 and B5) are attached on the B_5O_{12} unit, bridging with two BO_3 groups via corner sharing into a $[B_7O_{16}(OH)_2]^{13-}$ polyanion (Figure 1b). The $B_7O_{16}(OH)_2$ units are further interconnected by GeO_4 tetrahedra via Ge–O–B bridges to form a novel 3D anionic network with 1D 10-MR tunnels along the *b* axis (Figure 1a). The long and narrow-shaped helical tunnels are based on Ge_2B_8 10-MRs composed of two GeO_4, two BO_3, two $BO_3(OH)$, and four BO_4 polyhedra. The walls of the 10-MR tunnels are built from 14-MR windows (Figure S1 in the Supporting Information). Each 10-MR tunnel is surrounded by six other 10-MR tunnels as its neighbors. The 10-MR tunnel is filled with Ba2, Ba3, hydroxyl

dx.doi.org/10.1021/ic1025697 |*Inorg. Chem.* 2011, 50, 3037–3043

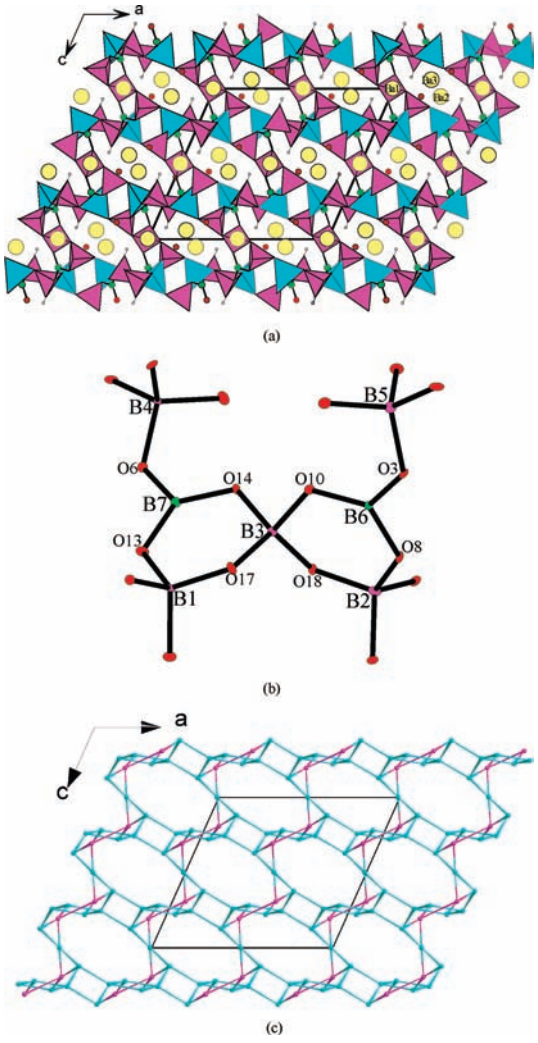

Figure 1. (a) View of the structure of $Ba_3[Ge_2B_7O_{16}(OH)_2](OH)(H_2O)$ with 1D 10-MR tunnels down the *b* axis. The GeO_4 and BO_4 tetrahedra are shaded in cyan and pink, respectively. The three-coordinated B, Ba, and O atoms are drawn as green, yellow, and red circles, respectively. (b) $B_7O_{16}(OH)_2$ unit shown in a thermal ellipsoid plot. (c) Topological view of a 3D new 5-nodal net with a Schläfli symbol of $\{3.4.8^2.9^2\}_2\{3.8.9\}_2\{3^2.10^2.11^2\}\{4.8^2\}_2\{4^2.8^2.10^2\}$. The pink and cyan balls represent the three- and four-connected nodes, respectively.

groups, and lattice water molecules, whereas Ba1 cations are located at the 14-MR windows of the 10-MR tunnels (Figure 1a).

Ba1 is 12-coordinated, whereas Ba2 and Ba3 are 11-cootdinated. The Ba−O distances are in the range of 2.560(6)−3.262(5) Å. Bond-valence calculations indicate that Ge and B atoms are in oxidation states of 4+ and 3+, respectively. The calculated total bond valences for Ge1, Ge2, B1, B2, B3, B4, B5, B6, and B7 are 3.98, 4.08, 3.01, 3.05, 3.11, 3.01, 2.96, 3.01, and 3.02, respectively.[17] It also should be noted that the hydroxyl group (O1H) forms relatively shorter Ba−O bonds [av 2.609(5) Å] with Ba^{II} cations compared with other Ba−O bonds [av 2.984(5) Å]. In addition to forming three long Ba−O bonds, O1W is also involved in hydrogen bonding with O2 and O6 with O···O separations of 2.685(7) and 2.839(7) Å, respectively. This could explain the unusual high thermal stability for this compound. $Ba_3[B_7Ge_2O_{16}(OH)_2](OH)(H_2O)$ also exhibits 1D Ge_2B_8 10-MR tunnels down the [110] and [−1−10] directions (Figure S2a,b in the Supporting Information).

As was mentioned earlier, the Ge atoms in the anionic framework of $Ba_3[B_7Ge_2O_{16}(OH)_2](OH)(H_2O)$ are four-coordinated and the B atoms are three- or four-coordinated. The three- and four-coordinated atoms act as three- and four-connected nodes, respectively. From a topological viewpoint, the 3D anionic network of $Ba_3[B_7Ge_2O_{16}(OH)_2](OH)(H_2O)$ can also be described as a new 5-nodal topological type with a Schläfli symbol of $\{3.4.8^2.9^2\}_2\{3.8.9\}_2\{3^2.10^2.11^2\}\{4.8^2\}_2\{4^2.8^2.10^2\}$ (Figure 1c). The Schläfli symbol for each node is as follows: B1, B2, $\{3.4.8^2.9^2\}$; B3, $\{3^2.10^2.11^2\}$; B4, B5, $\{4.8^2\}$; B6, B7, $\{3.8.9\}$, and Ge1, Ge2, $\{4^2.8^2.10^2\}$. In addition, it is interesting to mention that such a 5-nodal net is an augmented version of a new 3,4-c-binodal topological type with a Schläfli symbol of $\{6.8^2\}$-$\{6^4.8^{10}\}$ (Figure S3 in the Supporting Information).

The structure of $Ba_3Ge_2B_6O_{16}$ also belongs to a new structure type, and it features a novel thick anionic layer composed of cyclic B_6O_{16} units that are bridged by Ge atoms. Such an anionic thick layer contains 6-MR tunnels along the *a* axis, which are filled with Ba1 cations. Such neighboring layers are separated by Ba2 cations (Figure 2a). The asymmetric unit of $Ba_3Ge_2B_6O_{16}$ contains two Ba, one Ge, and three B atoms. The Ba1 atom is located at a site of the inversion center, whereas all other atoms occupy general sites. The Ge^{IV} atom is tetrahedrally coordinated by four O atoms, with Ge−O distances ranging from 1.718(4) to 1.753(5) Å and O−Ge−O bond angles in the range of 104.1(2)−115.1(2)°. B1 and B2 are tetrahedrally coordinated, whereas B3 is three-coordinated with a triangular BO_3 geometry. The B−O bond distances of the BO_3 group [1.327(8)−1.415(9) Å] are significantly shorter than those of BO_4 tetrahedra [1.439(9)−1.512(8) Å]. The O−B−O angles are in the ranges of 115.5(6)−123.5(6)° for triangular $B(3)O_3$ units and 103.1(5)−114.0(5)° for BO_4 tetrahedra. All of these distances and angles are comparable to those reported in other borogermanates.[4−13]

In the unit of B_6O_{16}, a pair of BO_4 tetrahedra are interconnected via corner sharing (O5) into a B_2O_7 dimer with a B1−O5−B2 bond angle of 130.4(5)°. Two B_2O_7 dimers are bridged by two triangular BO_3 groups via corner sharing in a novel cyclic B_6O_{16} unit. The distance between the O atoms across this ring is 3.420(9) Å (Figure 2b). To the best of our knowledge, such a type of borate unit has not been reported previously. The above B_6O_{16} units are further bridged by GeO_4 tetrahedra via corner sharing in a novel two-dimensional (2D) layer parallel to the *ac* plane (Figure 2c). The B−O−Ge angle is in the range of 125.0(4)−139.4(4)°. Such a type of $[Ge_2B_6O_{16}]^{6-}$ layer has not been reported yet. Viewed down the *a* axis, there are 1D tunnels of B_6 rings along the *a* axis, which are filled with Ba1 ions. The Ba2 cations are located at the interlayer space (Figure 2a). Ba1 is 10-coordinated by 10 O atoms, whereas Ba2 is 11-coordinated. The Ba−O distances are in the range of 2.659(5)−3.325(4) Å. Bond-valence calculations indicate that the B atoms are in an oxidation state of 3+ and the Ge atom is 4+, and the calculated total bond valences for B1, B2, B3, and Ge1 are 3.05, 3.00, 2.96, and 4.15, respectively.[17] Packing of the above 2D layers also resulted in 1D tunnels of 8-MRs along the *b* axis, which are filled with both Ba1 and Ba2 cations (Figure S4 in the Supporting Information). Each 8-MR contains two GeO_4 and four BO_4 tetrahedra as well as two BO_3 groups.

As was mentioned earlier, within the anionic layer of $[Ge_2B_6O_{16}]^{6-}$, Ge atoms are four-coordinated and B atoms are three- or four-coordinated. The tetrahedrally coordinated Ge

dx.doi.org/10.1021/ic1025697 |*Inorg. Chem.* 2011, 50, 3037–3043

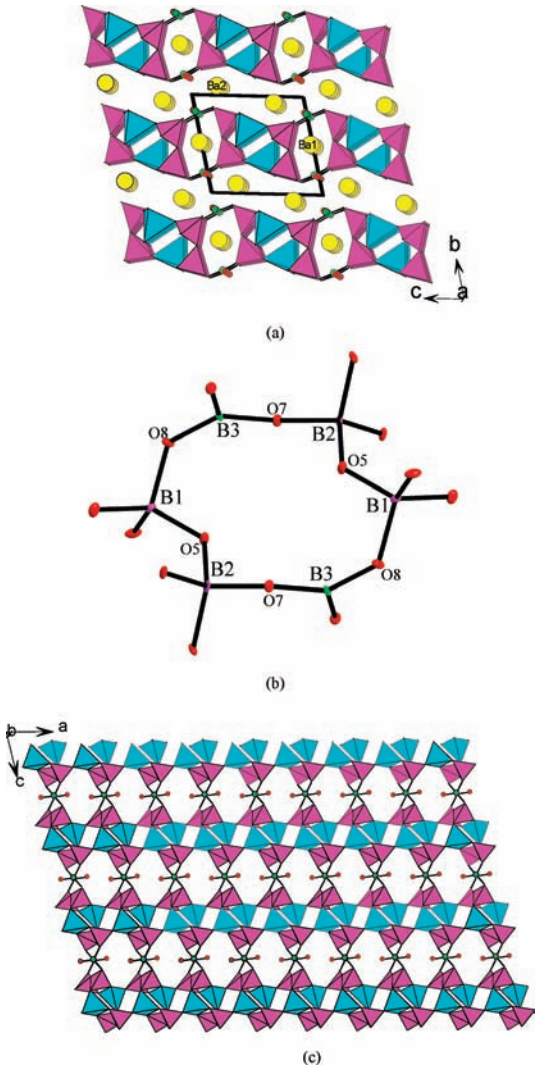

Figure 2. (a) Views of the structure of $Ba_3Ge_2B_6O_{16}$ down the *a* axis. (b) B_6O_{16} unit shown in a thermal ellipsoid plot. (c) 2D layer of $[Ge_2B_6O_{16}]^{6-}$ anions in $Ba_3Ge_2B_6O_{16}$. The GeO_4 and BO_4 tetrahedra are shaded in cyan and pink, respectively. The three-coordinated B and O atoms are drawn as green and red circles, respectively.

and B atoms act as two kinds of independent four-connected nodes, whereas the three-coordinated BO_3 units are merely linkers. From a topological viewpoint, the anionic layer of $[Ge_2B_6O_{16}]^{6-}$ can also be described as a new 4,4-c-binodal topological type with a Schläfli symbol of $\{4^3.6^3\}_2\{4^6.6^6.8^3\}$ (Figure S5 in the Supporting Information). The point symbol for BO_4 is $\{4^3.6^3\}$, whereas that for GeO_4 is $\{4^6.6^6.8^3\}$.

Optical Properties. Optical diffuse-reflectance spectral studies indicate that both $Ba_3[B_7Ge_2O_{16}(OH)_2](OH)(H_2O)$ and $Ba_3Ge_2B_6O_{16}$ are insulators with optical band gaps of 5.53 and 5.12 eV, respectively (Figure S8 in the Supporting Information). UV absorption spectra of $Ba_3[B_7Ge_2O_{16}(OH)_2](OH)(H_2O)$ and $Ba_3Ge_2B_6O_{16}$ revealed that they are transparent in the range of 350−2500 nm (Figure S9 in the Supporting Information). IR studies indicate that $Ba_3Ge_2B_6O_{16}$ shows no absorption bands in the range of 4000−1700 cm^{-1} (2.5−5.9 μm) and $Ba_3[B_7Ge_2O_{16}(OH)_2](OH)(H_2O)$ shows a few absorption bands in this range because of the presence of hydroxyl groups as well as water molecules. Hence, $Ba_3Ge_2B_6O_{16}$ is transparent in the range of

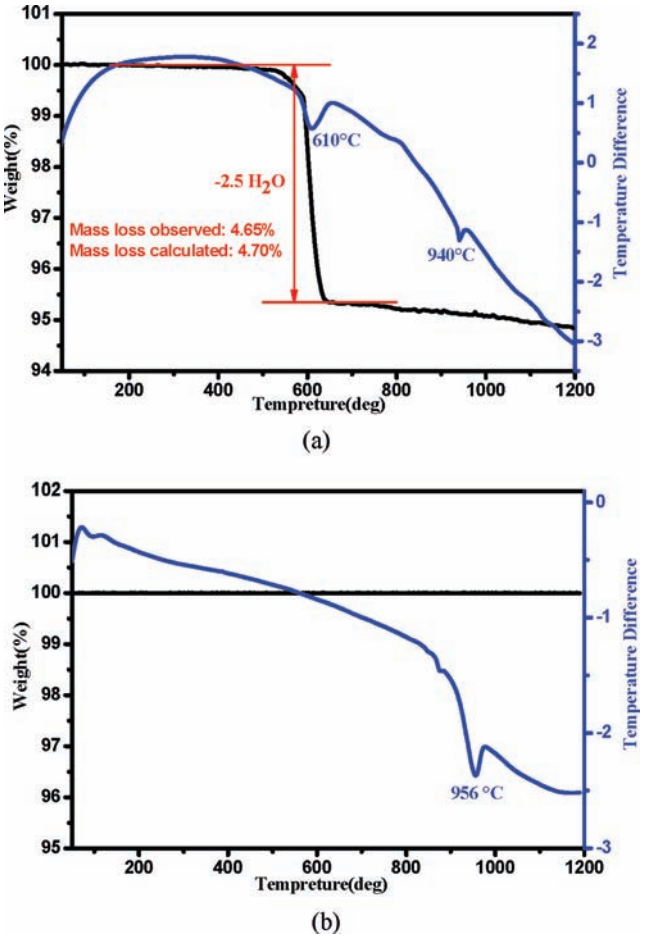

Figure 3. TGA and DTA curves for $Ba_3[Ge_2B_7O_{16}(OH)_2](OH)(H_2O)$ (a) and $Ba_3Ge_2B_6O_{17}$ (b).

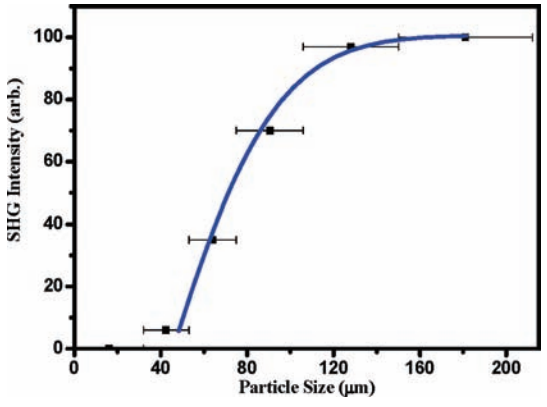

Figure 4. Phase-matching curves for $Ba_3[Ge_2B_7O_{16}(OH)_2](OH)(H_2O)$. The curve drawn is to guide the eye and not fit to the data.

0.35−5.9 μm. The IR spectra of the two compounds display strong absorption bands at 1228−1399 cm^{-1} that can be assigned to the asymmetrical stretch of the BO_3 groups. The bands for the BO_4 groups appear at 916−1131 cm^{-1}. The absorption peaks at 770−868 cm^{-1} can be assigned to the asymmetrical stretch of the GeO_4 groups. The absorption bands from 460 to 490 cm^{-1} correspond to the bending vibrations of the Ge−O bonds. The bending vibrations of BO_3 and BO_4 are also shown in

dx.doi.org/10.1021/ic1025697 |*Inorg. Chem.* 2011, 50, 3037–3043

Table 3. State Energies (eV) of the L-CB and H-VB of the Crystals $Ba_3[Ge_2B_7O_{16}(OH)_2](OH)(H_2O)$ and $Ba_3Ge_2B_6O_{16}$

compound	*k* point	L-CB	H-VB
$Ba_3[Ge_2B_7O_{16}(OH)_2](OH)(H_2O)$	L (−0.500, 0.000, 0.500)	4.926 91	−0.011 4
	M (−0.500, −0.500, 0.500)	5.042 67	−0.142 31
	A (−0.500, 0.000, 0.000)	4.930 65	−0.022 2
	G (0.000, 0.000, 0.000)	4.033 34	0
	Z (0.000, −0.500, 0.500)	4.926 92	−0.011 4
	V (0.000, 0.000, 0.500)	4.393 68	−0.045 51
$Ba_3Ge_2B_6O_{16}$	G (0.000, 0.000, 0.000)	3.783 94	−0.125 15
	F (0.000, 0.500, 0.000)	4.404 4	−0.220 45
	Q (0.000, 0.500, 0.500)	4.621 92	−0.084 55
	Z (0.000, 0.000, 0.500)	4.332 35	0
	G (0.000, 0.000, 0.000)	3.783 94	−0.125 15

400−700 cm^{-1}.[21] For $Ba_3[B_7Ge_2O_{16}(OH)_2](OH)(H_2O)$, the broad bands centered at 3161 and 1626 cm^{-1} can be assigned to stretching and bending modes of the O−H bonds, respectively (Figure S7 in the Supporting Information). These assignments are consistent with those previously reported.[5,10,11,13]

TGA and Differential Thermal Analysis (DTA) Studies. TGA studies indicate that there is no weight loss before 530 and 1200 °C, respectively for $Ba_3[B_7Ge_2O_{16}(OH)_2](OH)(H_2O)$ and $Ba_3Ge_2B_6O_{16}$ (Figure 3). $Ba_3[B_7Ge_2O_{16}(OH)_2](OH)(H_2O)$ exhibits one step of weight loss in the range of 530−640 °C, which corresponds to the release of 2.5 mol of water molecules per formula unit. The observed weight loss of 4.65% matches well with the calculated one (4.70%). This assignment is also in agreement with the endothermic peak at 610 °C in the DTA diagram. After dehydration, the compound becomes amorphous and loses weight slowly in the range of 640−1200 °C. The total weight loss at 1200 °C is 5.2%. The endothermic peak at 940 °C corresponds to the melting of the dehydrated product. For $Ba_3Ge_2B_6O_{16}$, there is no obvious weight loss before 1200 °C, indicating that it is thermally very stable. The endothermic peak at 956 °C corresponds to the melting of the compound.

SHG and Ferroelectric Properties. $Ba_3[B_7Ge_2O_{16}(OH)_2](OH)(H_2O)$ crystallized in the polar space group *Cc*; therefore, it is worth examining its SHG and ferroelectric properties. SHG measurements on a Q-switched Nd:YAG laser with sieved powder samples (70−100 mesh) revealed that $Ba_3[B_7Ge_2O_{16}(OH)_2](OH)(H_2O)$ displays a weak SHG response of approximately 0.3 times that of KDP, giving further evidence of the noncentrosymmetry of the structure. Furthermore, the results of the SHG efficiency versus particle size experiments indicate that the material is phase-matchable (Figure 4). The relatively weak SHG response may be attributed to the racemic twinning for its crystalline sample.

The ferroelectric property experiments revealed that there is an electric hysteresis loop in $Ba_3[B_7Ge_2O_{16}(OH)_2](OH)(H_2O)$ with a small remnant polarization (P_r) of 0.022 nC/cm^2, a coercive field (E_c) of 1280 V/cm, and a saturation spontaneous polarization (P_s) of 0.035 nC/cm^2 (Figure S10 in the Supporting Information). These coefficients are very small, and hence its ferroelectric property is negligible.

Theoretical Studies. The calculated band structures of $Ba_3[B_7Ge_2O_{16}(OH)_2](OH)(H_2O)$ and $Ba_3Ge_2B_6O_{16}$ are plotted in Figure S11 in the Supporting Information, and the state energies of the lowest conduction band (L-CB) and the highest valence band (H-VB) at high-symmetry points of the first Brillouin zone are listed in Table 3. It is clear that $Ba_3[B_7Ge_2O_{16}(OH)_2](OH)(H_2O)$ is a direct band-gap insulator (from G to G) with a band gap of 4.03 eV. For $Ba_3Ge_2B_6O_{16}$, the L-CB is at the G point and the H-VB is at the Z point. Thus, it is an indirect band-gap crystal with a band gap of 3.91 eV. The calculated band gaps are significantly smaller than the experimental ones [5.53 eV for $Ba_3[B_7Ge_2O_{16}(OH)_2](OH)(H_2O)$ and 5.12 eV for $Ba_3Ge_2B_6O_{16}$]. This is not surprising because it is well-known that the GGA does not accurately describe the eigenvalues of the electronic states, which causes a quantitative underestimation of the band gaps, especially for insulators.[22]

The bands can be assigned according to the total and partial DOS, as plotted in Figure S12 in the Supporting Information. It is found that the DOS curves of the two compounds are very similar; hence, we take $Ba_3[B_7Ge_2O_{16}(OH)_2](OH)(H_2O)$ as the example to describe them in detail. For $Ba_3[B_7Ge_2O_{16}(OH)_2](OH)(H_2O)$, the bottommost VB region near −25.0 eV comes from Ba 6s states, and the VBs ranging from −21.6 to −15.8 eV mainly originate from O 2s mixing with some B 2s2p states. Ba 5p states contribute to the peak near −10.3 eV. Near the Fermi level region, namely, −9.1−0 eV in VB and 4.4−10.4 eV in CB, O 2p states overlap with Ge 4p and B 2p, indicative of the covalent interactions of the B−O and Ge−O bonds.

Population analyses allow for a more quantitative bond analysis (Table S1 in the Supporting Information). The calculated bond orders of the B−O and Ge−O bonds are 0.56−0.95 and 0.47−0.56 e, respectively (a covalent single bond order is generally 1.0 e); hence, we can say that the B−O bonds are stronger than the Ge−O bonds. In addition, the bond orders of the B−O bonds in the BO_3 groups (0.73−0.95 e) are significantly larger than those in the BO_4 groups (0.56−0.72 e). The bond orders of the Ba−O bonds are much smaller (−0.09 to +0.18 e); these bonds are mainly ionic in nature.

CONCLUSIONS

In summary, two new barium borogermanates with two new types of structures, namely, $Ba_3[Ge_2B_7O_{16}(OH)_2](OH)(H_2O)$ and $Ba_3Ge_2B_6O_{16}$, have been synthesized by hydrothermal or high-temperature solid-state reactions. They represent the first examples of alkaline-earth borogermanates. $Ba_3[Ge_2B_7O_{16}(OH)_2](OH)(H_2O)$ features a novel 3D anionic framework composed of $[B_7O_{16}(OH)_2]^{13-}$ polyanions that are bridged by Ge atoms, whereas $Ba_3Ge_2B_6O_{16}$ shows a 2D layer structure based on B_6O_{16} units interconnected by GeO_4 tetrahedra. $Ba_3[Ge_2B_7O_{16}(OH)_2](OH)(H_2O)$ shows a weak SHG response of

dx.doi.org/10.1021/ic1025697 |*Inorg. Chem.* 2011, 50, 3037–3043

about 0.3 times that of KDP, and it is phase-matchable. The results of our studies indicate that inclusion of the germanate group into the borate system not only can enrich the structural chemistry of metal borates but also may afford new SHG materials. Our future research efforts will be devoted to the preparations of other boron-rich borogermanates with enhanced SHG properties by inclusion of a lone pair containing Pb^{2+} and Bi^{3+} cations or transition-metal ions with d^0 electronic configurations such as Ti^{4+}, V^{5+}, and Mo^{6+}, etc., both of which are susceptible to the second-order Jahn−Teller distortion.

■ ASSOCIATED CONTENT

Supporting Information. X-ray crystallographic files in CIF format, calculated bond orders, simulated and experimental powder XRD patterns, IR spectra, UV spectra, optical diffuse reflectance, electric hysteresis loops, bond structures, and DOS diagrams. This material is available free of charge via the Internet at http://pubs.acs.org.

■ AUTHOR INFORMATION

Corresponding Author
*E-mail: mjg@fjirsm.ac.cn. Fax: (+86)591-83714946.

■ ACKNOWLEDGMENT

This work was supported by the National Natural Science Foundation of China (Grants 20731006, 20825104, 21001107, and 20821061) and Key Project of FJIRSM (Grant SZD07001-2).

■ REFERENCES

(1) (a) Chen, C. T.; Liu, G. Z. *Annu. Rev. Mater. Sci.* **1986**, *16*, 203. (b) Chen, C. T.; Wu, B. C.; Jiang, A. D.; You, G. M. *Sci. Sin., Ser. B* **1985**, *18*, 235. (c) Chen, C. T.; Wu, Y. C.; Jiang, A. D.; Wu, B. C.; You, G. M.; Li, R. K.; Lin, S. J. *J. Opt. Soc. Am. B* **1989**, *6*, 616. (d) Wu, Y. C.; Sasaki, T.; Nakai, S.; Yokotani, A.; Tang, H. G.; Chen, C. T. *Appl. Phys. Lett.* **1993**, *62*, 2614.

(2) (a) Wang, S. C.; Ye, N.; Li, W.; Zhao, D. *J. Am. Chem. Soc.* **2010**, *132*, 8779. (b) Zhang, W. L.; Cheng, W. D.; Zhang, H.; Geng, L.; Lin, C. S.; He, C. Z. *J. Am. Chem. Soc.* **2010**, *132*, 1508. (c) Huang, Y. Z.; Wu, L. M.; Wu, X. T.; Li, L. H.; Chen, L.; Zhang, Y. F. *J. Am. Chem. Soc.* **2010**, *132*, 12788.

(3) (a) Bu, X.; Feng, P.; Stucky, G. D. *J. Am. Chem. Soc.* **1998**, *120*, 11204. (b) Bu, X.; Feng, P.; Gier, T. E.; Zhao, D.; Stucky, G. D. *J. Am. Chem. Soc.* **1998**, *120*, 13389. (c) Beitone, L.; Loiseau, T.; Férey, G. *Inorg. Chem.* **2002**, *41*, 3962. (d) Cascales, C.; Gutiérrez-Puebla, E.; Monge, M. A.; Ruíz-Valero, C. *Angew. Chem., Int. Ed.* **1998**, *37*, 129.

(4) (a) Dadachov, M. S.; Sun, K.; Conradsson, T.; Zou, X. D. *Angew. Chem., Int. Ed.* **2000**, *39*, 3674. (b) Li, Y.; Zou, X. D. *Angew. Chem., Int. Ed.* **2005**, *44*, 2012. (c) Li, Y. F.; Zou, X. D. *Acta Crystallogr.* **2003**, *C59*, 471.

(5) (a) Pan, C. Y.; Liu, G. Z.; Zheng, S. T.; Yang, G. Y. *Chem.—Eur. J.* **2008**, *14*, 5057. (b) Wang, G. M.; Sun, Y. Q.; Yang, G. Y. *Cryst. Growth Des.* **2005**, *5*, 313. (c) Zhang, H. X.; Zhang, J.; Zheng, S. T.; Yang, G. Y. *Inorg. Chem.* **2005**, *44*, 1166. (d) Cao, G. J.; Fang, W. F.; Zheng, S. T.; Yang, G. Y. *Inorg. Chem. Commun.* **2010**, *13*, 1047.

(6) Zhang, J. H.; Li, P. X.; Mao, J. G. *Dalton Trans.* **2010**, *39*, 5301.

(7) Heymann, G.; Huppertz, H. *J. Solid State Chem.* **2006**, *179*, 370.

(8) Ilyukhin, A. B.; Dzhurinskii, B. F. *Russ. J. Inorg. Chem.* **1994**, *39*, 530.

(9) (a) Kaminskii, A. A.; Mill, B. V.; Belokoneva, E. L.; Butashin, A. V. *Izv. Akad. Nauk SSSR, Neorg. Mater.* **1990**, *26*, 1105. (b) Belokoneva, E. L.; Mill, B. V.; Butashin, A. V.; Kaminskii, A. A. *Izv. Akad. Nauk SSSR, Neorg. Mater.* **1991**, *27*, 1700.

(10) (a) Lin, Z. E.; Zhang, J.; Yang, G. Y. *Inorg. Chem.* **2003**, *42*, 1797. (b) Zhang, H. X.; Zhang, J.; Zheng, S. T.; Wang, G. M.; Yang, G. Y. *Inorg. Chem.* **2004**, *43*, 6148.

(11) Kong, F.; Jiang, H. L.; Hu, T.; Mao, J. G. *Inorg. Chem.* **2008**, *47*, 10611.

(12) (a) Xiong, D. B.; Zhao, J. T.; Chen, H. H.; Yang, X. X. *Chem.—Eur. J.* **2007**, *13*, 9862. (b) Xiong, D. B.; Chen, H. H.; Li, M. R.; Yang, X. X.; Zhao, J. T. *Inorg. Chem.* **2006**, *45*, 9301.

(13) (a) Parise, J. B.; Gier, T. E. *Chem. Mater.* **1992**, *4*, 1065. (b) Kaminskii, A. A.; Becker, P.; Bohaty, L.; Bagaev, S. N.; Eichler, H. J.; Ueda, K.; Hanuza, J.; Rhee, H.; Yoneda, H.; Takaichi, K.; Terashima, I.; Maczka, M. *Laser Phys.* **2003**, *11*, 1385.

(14) Wendlandt, W. M.; Hecht, H. G. *Reflectance Spectroscopy*; Interscience: New York, 1966.

(15) Kurtz, S. W.; Perry, T. T. *J. Appl. Phys.* **1968**, *39*, 3798.

(16) (a) *CrystalClear*, version 1.3.5; Rigaku Corp.: Woodlands, TX, 1999. (b) Sheldrick, G. M. *SHELXTL, Crystallographic Software Package*, version 5.1; Bruker-AXS: Madison, WI, 1998.

(17) (a) Brown, I. D.; Altermatt, D. *Acta Crystallogr.* **1985**, *B41*, 244. (b) Brese, N. E.; O'Keeffe, M. *Acta Crystallogr.* **1991**, *B47*, 192.

(18) (a) Segall, M. D.; Lindan, P. J. D.; Probert, M. J.; Pickard, C. J.; Hasnip, P. J.; Clark, S. J.; Payne, M. C. *J. Phys.: Condens. Matter* **2002**, *14*, 2717. (b) Milman, V.; Winkler, B.; White, J. A.; Pickard, C. J.; Payne, M. C.; Akhmatskaya, E. V.; Nobes, R. H. *Int. J. Quantum Chem.* **2000**, *77*, 895.

(19) Perdew, J. P.; Burke, K.; Ernzerhof, M. *Phys. Rev. Lett.* **1996**, *77*, 3865.

(20) Lin, J. S.; Qteish, A.; Payne, M. C.; Heine, V. *Phys. Rev. B* **1993**, *47*, 4174.

(21) Nakamoto, K. *Infrared Spectra of Inorganic and Coordination Compounds*; Wiley: New York, 1970.

(22) (a) Godby, R. W.; Schluther, M.; Sham, L. J. *Phys. Rev. B* **1987**, *36*, 6497. (b) Okoye, C. M. I. *J. Phys.: Condens. Matter* **2003**, *15*, 5945. (c) Terki, R.; Bertrand, G.; Aourag, H. *Microelectron. Eng.* **2005**, *81*, 514. (d) Jiang, H. L.; Kong, F.; Mao, J. G. *J. Solid State Chem.* **2007**, *180*, 1764.